Interference-Resilient Ultra-Low Power Aperiodic Data Collection

Timofei Istomin
University of Trento, Italy
Bruno Kessler Foundation, Italy
timofei.istomin@unitn.it

Matteo Trobinger
University of Trento, Italy
matteo.trobinger@unitn.it

Amy L. Murphy
Bruno Kessler Foundation, Italy
murphy@fbk.eu

Gian Pietro Picco
University of Trento, Italy
gianpietro.picco@unitn.it

ABSTRACT

Aperiodic data collection received little attention in wireless sensor networks, compared to its periodic counterpart.

The recent Crystal system uses synchronous transmissions to support aperiodic traffic with near-perfect reliability, low latency, and ultra-low power consumption. However, its performance is known under mild interference—a concern, as Crystal relies heavily on the (noise-sensitive) capture effect and targets aperiodic traffic where "every packet counts".

We exploit a 49-node indoor testbed where, in contrast to existing evaluations using only *naturally* present interference to evaluate synchronous systems, we rely on JamLab to *generate* noise patterns that are not only more disruptive and extensive, but also *reproducible*. We show that a properly configured, unmodified Crystal yields perfect reliability (unlike Glossy) in several noise scenarios, but cannot sustain extreme ones (e.g., an emulated microwave oven near the sink) that instead are handled by routing-based approaches. We extend Crystal with techniques known to mitigate interference—channel hopping and noise detection—and demonstrate that these allow Crystal to achieve performance akin to the original even under multiple sources of strong interference.

CCS CONCEPTS

• **Networks → Network protocol design**;

KEYWORDS

Synchronous transmissions, wireless sensor networks, energy efficiency, interference resilience, channel hopping.

ACM Reference Format:
Timofei Istomin, Matteo Trobinger, Amy L. Murphy, and Gian Pietro Picco. 2018. Interference-Resilient Ultra-Low Power Aperiodic Data Collection. In *Proceedings of ACM Conference (Conference'17).* ACM, New York, NY, USA, 12 pages. https://doi.org/10.1145/nnnnnnn.nnnnnnn

Permission to make digital or hard copies of all or part of this work for personal or classroom use is granted without fee provided that copies are not made or distributed for profit or commercial advantage and that copies bear this notice and the full citation on the first page. Copyrights for components of this work owned by others than ACM must be honored. Abstracting with credit is permitted. To copy otherwise, or republish, to post on servers or to redistribute to lists, requires prior specific permission and/or a fee. Request permissions from permissions@acm.org.
Conference'17, July 2017, Washington, DC, USA
© 2018 Association for Computing Machinery.
ACM ISBN 978-x-xxxx-xxxx-x/YY/MM…$15.00
https://doi.org/10.1145/nnnnnnn.nnnnnnn

1 INTRODUCTION

Aperiodic data collection received little attention in wireless sensor networks, compared to its periodic counterpart. A notable exception is our Crystal system, recently proposed in [15]. Originally designed to exploit the synergy with data prediction, Crystal uses synchronous transmissions [8] to support *aperiodic* and *sparse* traffic with near-perfect reliability, low latency, and ultra-low power consumption.

Is Crystal resilient to strong interference? However, the remarkable performance of Crystal was reported only under mild interference; we ran experiments on channel 20 and 26 which *"showed very similar performance [...] during the night runs; however, the daytime results were inconsistent and difficult to assess"* and therefore *"the results only from night runs on channel 26"* were included [15].

Statements like these are not uncommon in the related literature, as discussed later. However, this is of particular concern here because interference *i)* potentially undermines Crystal at the core by hampering the capture effect it heavily relies on, and *ii)* increases the overhead of achieving near-perfect reliability of aperiodic and sparse traffic in which "every packet counts", possibly precluding ultra-low power consumption.

Hence, whether the remarkable performance in [15] holds under strong interference is an open question, answered in this paper by analyzing the performance of Crystal under several, increasingly disruptive noise patterns and introducing techniques to boost its resilience to strong interference without sacrificing ultra-low power consumption.

Natural vs. Generated Interference. We report experiments in a 49-node indoor testbed and exploit its *natural* interference, mostly WiFi, in line with the evaluation of well-known synchronous transmissions systems [8, 9, 16, 27].

Actually, reliance on natural interference is the *only* methodology hitherto adopted for evaluating them. Despite Glossy and derivatives being commonly considered highly resilient to interference, the extent to which this holds has never been ascertained under noise patterns that are *i) repeatable*, and *ii)* more extensive and disruptive than natural ones.

We raise the standard of evaluating synchronous transmissions under interference by reporting, for the first time, results based on the *reproducible generation* of realistic noise patterns. We use JamLab [1], described in §2, to emulate WiFi devices and microwave ovens in our experimental setup (§3).

Performance Metrics and Comparison Baselines. We evaluate CRYSTAL using packet delivery rate (*PDR*) and duty cycle (*DC*) as metrics for reliability and energy consumption, respectively. Moreover, as CRYSTAL relies on unmodified Glossy, we indirectly evaluate it with the same experiments under interference; as mentioned above, we argue this is a contribution per se.

We observe that none of the proposals tackling interference found its way into the mainstream. Hence, we choose the readily-available RPL [25] and ORPL [6] as baselines (§4), in line with analogous works [18, 20, 28].

Results and Contributions. We show (§5) that all protocols sustain natural interference, but only Glossy and CRYSTAL achieve near-perfect *PDR*, with a much lower *DC*. Under JamLab-emulated WiFi, RPL reliability degrades even with a single jammer; with several covering the entire testbed, ORPL also degrades, while CRYSTAL still achieves near-perfect *PDR*. Interestingly, roles are reversed when an emulated microwave oven is placed 1m from the sink; ORPL achieves near-perfect *PDR*, while CRYSTAL falls below 80%.

These results pushed us to explore two techniques to improve the resilience of CRYSTAL (§6). The first allows nodes to *escape* interference by executing each transmission-acknowledgement pair—a core CRYSTAL constituent—on different channels, based on a network-wide hopping sequence. This approach, which uses Glossy unmodified, is notably different from protocols in the literature that apply channel hoping *inside* Glossy [7, 17, 21]. Second, noise detection at all nodes enables them to schedule extra transmissions in a decentralized way, increasing packet delivery. This *fights* interference, effectively providing a "safety net" when channel hopping alone is insufficient, but may keep nodes unnecessarily active, which detrimental in the sparse traffic targeted by CRYSTAL.

Our experimental results (§7) show that the combination of these two techniques, to the best of our knowledge novel in the context of synchronous transmissions, achieves near-perfect reliability in the very challenging scenarios where *both* microwave ovens *and* WiFi are simultaneously present. Overall, we confirm that the original CRYSTAL (and the underlying Glossy) can tolerate the moderate levels of interference commonly found in office environments. However, CRYSTAL can also be modified with relative ease to sustain much stronger interference patterns while retaining its ultra-low power consumption.

Finally, we concisely survey related work (§8), before ending the paper with brief concluding remarks (§9).

2 BACKGROUND

We offer the necessary background on synchronous transmissions and CRYSTAL, along with the JamLab infrastructure used to generate reproducible interference patterns.

2.1 Synchronous Transmissions: CRYSTAL

Synchronous transmission protocols, pioneered by Glossy [8], build on two properties of the IEEE 802.15.4 PHY: constructive interference and capture effect. These occur when packet transmissions by neighboring nodes are initiated within a tiny temporal interval (0.5μs and 160μs, respectively) and yield a successful reception instead of a collision. Constructive interference works when the packet is the same, yielding high reliability due to the combination of the identical signals; the capture effect, instead, works with different packets, one of which is received with a probability depending on the density of neighbors and their signal strength.

Table 1: An aperiodic, sparse traffic profile; number and fraction of epochs with U concurrent senders.

	U	0	1	2	5	10	20
epochs	#	84.3K	15.5K	2.2K	606	46	1
	%	82.1	15.1	2.2	0.14	0.038	0.005

Glossy exploits these properties to construct network-wide floods that are extremely *i) fast*, as each node receiving a packet immediately rebroadcasts it, preserving the required tight timing *ii) reliable*, due to the above PHY-level properties, and the inherent spatial and temporal redundancy of flooding. To increase reliability, packets are retransmitted by each node N times; the value of N is the main knob to control the tradeoff between reliability and energy consumption.

Aperiodic, sparse data collection. CRYSTAL [15] builds a schedule atop Glossy that, unlike works geared towards periodic data collection [9, 24], is designed to efficiently support aperiodic, sparse traffic like the one stemming from applying data prediction [13, 22] to regular, periodic traffic. Prediction quenches the majority of application messages, inducing sporadic traffic interleaved with long, quiescent intervals. However, a sudden change in the monitored phenomena may invalidate the prediction model, which must be regenerated and sent to the sink, possibly by multiple nodes at once. Table 1, adapted from [15], shows an example traffic profile resulting from applying data prediction to the well-known 36-day Intel dataset [14] containing temperature samples gathered with a period of 30s, hereafter called *epoch*. After data prediction is applied, the majority (82.1%) of the total 102686 epochs is empty, as the sink can predict the next value based on the last model reported by each node. However, in a non-negligible fraction of epochs, $U > 1$ concurrent senders must send model updates. Further, as packets carry models rather than raw data, the loss of a single one has a much larger impact on the reliability of the overall system.

CRYSTAL in a nutshell. To reconcile these requirements, CRYSTAL builds a network-wide transport protocol, in which *i)* a transmission (T) slot is used by U concurrent senders to disseminate their packet; these floods "compete" until, thanks to the capture effect and Glossy redundancy, one reaches the sink with high probability *ii)* a subsequent acknowledgment (A) slot is used by the sink to flood the identifier of the sender whose packet it received, informing the others whether re-transmission is needed because their packet was "overcome" by another or no packet was received at the sink.

Figure 1 illustrates the concept in a simplified setting with only 2 nodes and the sink. A synchronization (S) phase is performed at the beginning of each epoch to ensure time synchronization. Communication occurs via the aforementioned TA pairs, which are repeated by fewer and fewer senders until all have successfully transmitted their packet and the entire network goes to sleep for the rest of the epoch. This termination condition is in principle easily identified by the first *silent pair*, i.e., one without transmissions in T and whose A contains a negative acknowledgment. In practice, matters are complicated by packet losses in either T or A, which may cause a node or the sink to become prematurely inactive. Therefore, CRYSTAL detects termination after R *consecutive* silent pairs; larger

Table 2: Crystal configurations used in the paper. The values of W_x and G are in milliseconds.

Power	N_S	N_T	N_A	W_S	W_T	W_A	G	R	Z
High	3	2	3	10	6	8	0.15	2	4
	3	3	3	10	8	8			
Low	3	3	3	12	10	10			
	4	4	4	14	12	12			

values improve reliability but with higher energy consumption. Other parameters are described in [15], e.g., the duration G of guards and the number Z of consecutive missed acknowledgements.

Baseline configuration. In essence, Crystal builds a reliability layer atop Glossy, which strikes different tradeoffs w.r.t. energy consumption by exploiting the interplay between the two layers. As in Glossy, the number N of retransmissions in each flood is key, but in Crystal this can be set independently (N_S, N_T, N_A) for each phase; the same holds for the maximum slot duration W, another key Glossy parameter.

The configuration used in the paper (Table 2) is adapted from the original. First, our testbed has a larger diameter than Indriya, used in [15]. This forced us to use larger values for the intervals W_T and W_A to allow Glossy floods to complete; we determined the optimal value using the methodology of [15]. Second, we experiment with combinations of N_T and N_A values to explore the impact of the T phase w.r.t. interference. The values of the remaining parameters W_S, G, R, Z are unchanged.

Finally, we use two power settings, high (0dBm) and low (−7dBm); the former is the default throughout the paper.

2.2 Generating Interference: JamLab

As we argued in §1, the ability to reproduce interference patterns is key to our study. Therefore, we rely on JamLab [1], which achieves this goal using the same mote-class nodes available in a testbed, and whose software faithfully emulates various types of interference relevant to IEEE 802.15.4, including Bluetooth, WiFi, and microwave ovens. These have very different characteristics. Bluetooth interferes with all IEEE 802.15.4 channels, as it uses a channel hopping scheme. WiFi spans 4 IEEE 802.15.4 channels with interference that is significantly stronger than Bluetooth, but also based on the type of data traffic. Microwave ovens, depending on model and load, may interfere with several consecutive channels, if not all, and induce very strong, continuous interference for 5-10ms, alternated with inactive periods of 10-15ms [1, 12]. According to [1], channels 20–26 are affected the most.

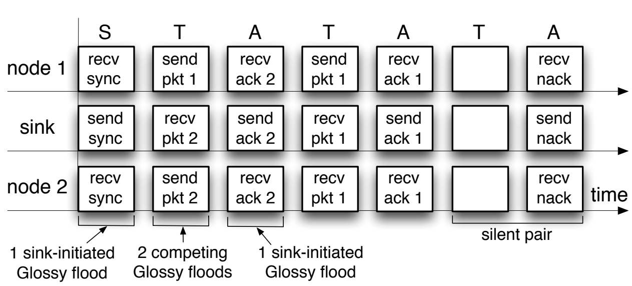

Figure 1: Crystal in a nutshell.

Hereafter, to put ourselves in the worst-case scenario, we focus only on WiFi and microwave ovens, as they yield the strongest interference. Similarly, we select the most challenging of the WiFi patterns offered by JamLab (JL_WIFI4) and configure the jammers to transmit modulated carrier at the maximum power (0dBm).

One criticism of JamLab is that the interference sources it can mimic are limited, and real environments may contain different ones. While this is true, the aforementioned characteristics of WiFi and microwave are different enough to cover a broad spectrum of noise patterns; further, by combining them, we create an even more challenging interference scenario for our experiments.

Another JamLab limitation is that real interference sources often interfere with many contiguous IEEE 802.15.4 channels at the same time; in contrast, a JamLab node generates noise on a single channel. The majority of the proposed protocols, including the synchronous transmissions ones described in §2.1 and the mainstream ones in §4, operate on a single channel; therefore this limitation does not affect the experiments in §5. However, in §7 we explore channel hopping and address this JamLab limitation with a channel mapping strategy.

Finally, although we use the maximum TX power (0dBm) of motes, this is much smaller than real interference sources (e.g., 25 and 60dBm for WiFi and microwave ovens, respectively). As suggested in [1], we use therefore *multiple* motes, strategically placed in our testbed (Figure 2).

3 TESTBED INTERFERENCE SCENARIOS

The experiments we report were performed in our local testbed, composed of 49 TMote Sky nodes deployed (Figure 2) in a 60×40 m^2 office area, subject to WiFi interference. Similar to other reports [18] the latter *i)* is more intense during the day and less at night and during the weekends, and *ii)* varies depending on the channel considered. In addition to this *natural* interference, we leverage controlled JamLab *generated* interference, enabling repeatable experiments. Overall, we define four types of interference (Table 3). The choice of channels for natural interference derives from an extensive, cross-channel measurement campaign, which identified the best (26) and worst (18) channels during night and day, respectively. The generated interference is created at night on channel 26 (i.e., under

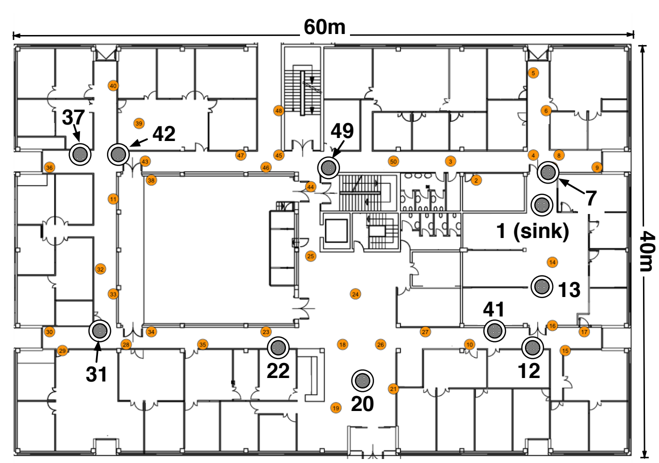

Figure 2: Position of the jammers in the testbed.

Table 3: Types of interference.

Type of interference		Description
Natural	T-LOW	testbed at night/weekends, channel 26
	T-HIGH	testbed during the day, channel 18
Generated	J-WIFI	JamLab WiFi interference (JL_WIFI4)
	J-MWO	JamLab microwave oven interference

natural T-LOW interference). Our evaluation uses varying numbers of JamLab jammers for each type and combines different types in the same experiments, to obtain challenging, realistic setups. Node 1 is the sink in all experiments.

Figure 3 quantitatively compares the various types of interference while Figure 4 shows its effect on the number of links, their qualities and the network radius (Glossy hopcount). The natural T-LOW (Figure 3a) exhibits an average noise of −93dBm, rather stable and uniform across the network. The interference in natural T-HIGH is drastically different (Figure 3b). The average noise is −88dBm, but several nodes are exposed to much higher noise, reaching −50dBm. This affects the network topology by reducing the number of perfect links by $^1/_3$, yielding a 10% increase in the average hopcount (Figure 4).

The interference generated via JamLab yields stronger noise than the natural one. Figure 3c shows the J-WIFI interference generated by node 7 alone, the closest (1m) to the sink. Figure 3d shows instead the effect of 6 J-WIFI jammers, including node 7, chosen to cover the entire testbed (Figure 2). Compared to Figure 3b, J-WIFI subjects the network to a noise slightly higher in average (−86dBm) and variance (Figure 3d); this affects significantly the network topology, increasing the average hopcount by 20% w.r.t. T-HIGH (Figure 4).

Figure 3e shows the noise generated by a J-MWO jammer on node 7. About $^1/_4$ of the network (obviously including the sink) is severely affected, with an average noise from −80 to −65dBm, far higher than the previous scenarios. We experiment with alternate placements of the J-MWO jammer which clearly affects differently the sink, but also has different global effects on the network (Figure 4). Moreover, we also experiment with the *combination* of 2 J-MWO and 4 J-WIFI; the resulting noise (Figure 3f) is significantly higher than in all previous scenarios, yielding a stronger impact on network topology (Figure 4). This scenario combined with a reduced TX power of the network nodes (LP in Figure 4) is the most challenging we consider in this paper. Further, when studying specific effects of different jammers and their combinations on protocols, to eliminate the topology bias, we stick to a single 43-node network with the remaining 6 nodes being either active as jammers or switched off. Obviously, the 43-node network is more challenging as it is less connected (Figure 4).

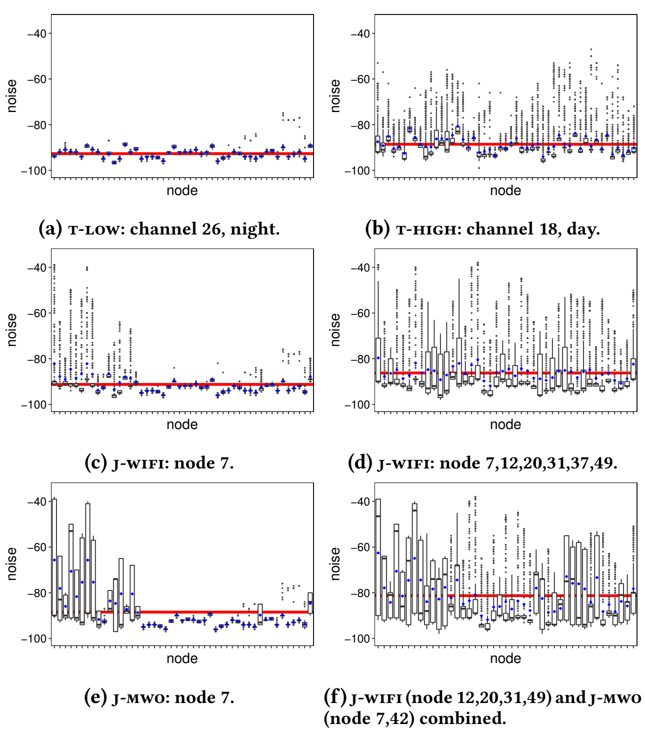

(a) T-LOW: channel 26, night.

(b) T-HIGH: channel 18, day.

(c) J-WIFI: node 7.

(d) J-WIFI: node 7,12,20,31,37,49.

(e) J-MWO: node 7.

(f) J-WIFI (node 12,20,31,49) and J-MWO (node 7,42) combined.

Figure 3: Noise levels for the scenarios in Table 3.

4 BASELINE MAINSTREAM PROTOCOLS

We describe the protocols we use as a baseline to compare against CRYSTAL, along with the configuration used in the experiments. All protocols in this paper run atop Contiki.

4.1 Protocol Descriptions

RPL [25], the Routing Protocol for Low-power Lossy Networks, is an IETF standard. RPL can be seen as an evolution of CTP [10] that, instead of a tree, maintains a directed acyclic graph rooted at the sink. Therefore, each node maintains multiple parents towards the

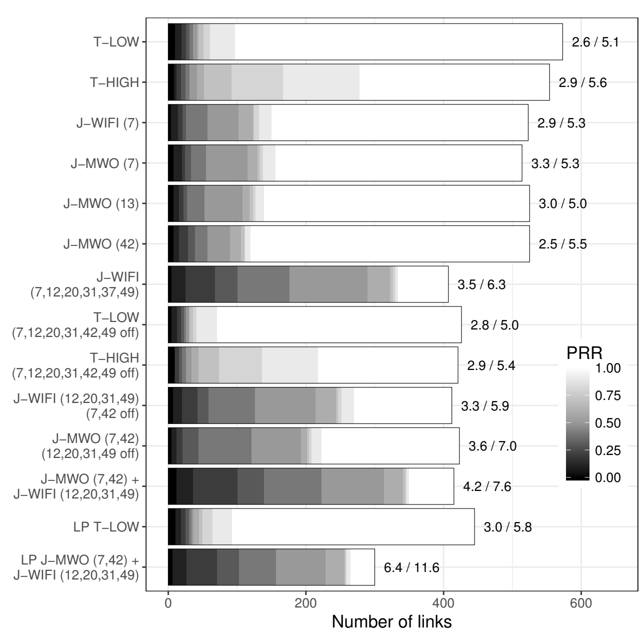

Figure 4: Link quality distribution (PRR) and network radius (mean/max) in various interference scenarios.

root; a preferred one is used for actual packet forwarding, while the others are kept as backup routes.

ORPL [6] is an opportunistic routing protocol that inherits many design choices from RPL but replaces unicast forwarding with anycast. Instead of relaying a packet to the parent, the forwarder broadcasts it; any neighbor closer to the sink is free to catch the packet, acknowledge it, and forward it in the same way. This increases resilience to interference; packets following different paths dynamically avoid noisy areas.

4.2 Protocol Configurations

MAC wake-up interval. Both protocols rely on ContikiMAC [4] for medium access control and duty cycling; the value of the wake-up interval is therefore a key parameter affecting performance. We initially chose a value of 8Hz; this is the default, commonly used in the literature. Although our goal in this paper is *not* to explore the best configuration of these mainstream protocols, we experimented also with values of 1, 2, 4 Hz, as they may provide better performance under interference. We observed this to be the case for ORPL, which performs best at 2Hz. Therefore, hereafter we report only about wake-up intervals of 2Hz and 8Hz; in general, these also strike a different balance between *PDR* and *DC*, and are therefore interesting to compare. The other configurations always perform worse, and are omitted due to space constraints.

Choosing the right CCA. The Clear Channel Assessment (CCA) mechanism is used by CSMA link layers to deter a packet transmission if the medium is busy. Its configuration significantly affects the interference resilience of the stack.

The CC2420 radio offers three modes where the CCA reports a busy medium upon detecting *1)* energy above threshold *2)* valid IEEE 802.15.4 data, regardless of energy threshold *3)* energy above threshold *or* valid IEEE 802.15.4 data.

We verified that the default −90dBm energy threshold in ContikiMAC yields unacceptable performance; baseline protocols achieve *PDR*<30% even with natural T-HIGH interference. We tested them with several values ranging from −60 to −90 dBm under T-HIGH and generated interference. The value of −77 dBm yielded the best performance and is our choice; in fact, this is the default for CC2420.

As for the CCA mode, the protocols considered use mode 3, the default. With JamLab nodes, the question arises whether the noise patterns they emit can be detected by other nodes as legit IEEE 802.15.4 data, instead of interference. We performed dedicated experiments comparing results obtained with CCA modes 1 and 3, observing essentially the same performance. Therefore, hereafter we used the default mode 3.

Retransmissions. RPL and ORPL employ different strategies w.r.t. layer 2 retransmissions; a maximum of 7 is allowed by RPL when an acknowledgment is not received, and 4 by ORPL. However, a retransmission can be triggered also by a CCA detecting a busy channel, in which case a few subtleties of the Contiki operating system come into play. Contiki v.3.0, used by RPL, considers 5 busy CCAs as equivalent to a failed transmission. The two events are completely unrelated in Contiki v.2.7, used by ORPL, allowing for an unlimited number of CCAs till the channel is free.

We did not modify these settings, as changing these *default* parameters may have unexpected and undesired effects whose analysis is outside the scope of this paper. We mention them here because they are useful in interpreting the results we present in the next section, e.g., the superior performance of ORPL under strong interference next to the sink.

5 CRYSTAL VS. THE MAINSTREAM

We compare the protocols in §4 against CRYSTAL, and indirectly Glossy, when exposed to the same interference. Aside from the intrinsic value and novelty of this experimental comparison, this serves a stepping stone towards a CRYSTAL design tolerating stronger interference, discussed in §6.

5.1 Experimental Setup

We analyze CRYSTAL and the baseline protocols in the interference scenarios described in §3. We setup a number U of concurrent senders between 0 and 48; $U=0$ means absence of traffic while $U=48$ offers a stress case where all nodes but the sink are senders. These parameters match the use cases described in [15] in which a data prediction scheme is applied to periodic data collection applications (e.g., sensing light in a road tunnel or temperature in an office environment). Data prediction reshapes traffic from periodic into sporadic; yet, in a single epoch, U nodes may need to transmit data. The *PDR* of Glossy is derived from CRYSTAL experiments as the *PDR* of the T phase when $U=1$ (Table 7).

In CRYSTAL, all U senders attempt their data packet transmission at exactly the same time, i.e., in the first T phase of the epoch, whose duration we set to $E=2$s. Baseline protocols have much higher latency, especially under interference; we set a longer $E=10$s for them, denoting solely the period according to which packets are generated. In reporting *DC*, we re-scale the values measured for CRYSTAL to 10s, to enable direct comparison between the two protocol classes. Unlike CRYSTAL, the epochs of baseline protocols are *not* synchronized.

Finally, all results are based on several 1-hour runs. For baseline protocols, these are preceded by a 30-minute period since bootstrap, allowing network topology to stabilize. For CRYSTAL, the total number of packets sent *per configuration* varied from 5000 to 500k, but typically was around 5k–40k. *PDR* is computed over the total number of packets sent. Instead, *DC* is the averaged over values from each 1-hour run, whose variation is anyway negligible.

5.2 Natural Interference: T-LOW

We first consider the T-LOW scenario (§3), which is akin to several evaluations in the literature, including [15], and offers a good baseline to compare higher interference against.

The performance of mainstream protocols in T-LOW (Table 4, left) is in line with experiments in the literature [6, 11]. As expected, the MAC wake-up interval bears a significant effect: RPL performs best at 8Hz, while ORPL achieves near-perfect *PDR* at 2Hz. Further, its *DC* is much lower than RPL thanks to opportunistic behavior.

These results were derived with a single sender, $U=1$. Table 6 shows results for other values of U; we consider only ORPL as the performance of RPL is significantly lower. The *PDR* of ORPL decreases when traffic increases; ORPL still achieves a good *PDR*= 97.8% with $U=20$, but drops to *PDR*=73% when all nodes transmit in each epoch. *DC* similarly increases sharply with U.

Table 4: Natural interference: Baseline, $U=1$.

		T-LOW		T-HIGH	
protocol	wake-up (Hz)	*PDR* (%)	*DC* (%)	*PDR* (%)	*DC* (%)
RPL	2	92.0	1.36	49.3	1.60
RPL	8	93.7	1.2	92.5	1.53
ORPL	2	99.8	0.380	98.2	0.71
ORPL	8	98.7	0.737	98.6	1.45

Table 5: Natural interference: Crystal.

			T-LOW		T-HIGH		
N_T	W_T	U	*PDR* (%)	*DC* (%)	*PDR* (%)	lost 1 pkt in	*DC* (%)
2	6	0	—	0.293	—	—	0.297
2	6	1	100	0.387	100	∞	0.396
2	6	2	100	0.479	100	∞	0.491
2	6	5	100	0.751	100	∞	0.773
2	6	10	100	1.205	99.9988	83659	1.233
2	6	20	100	2.107	99.9993	134077	2.162
2	6	48	100	4.883	100	∞	4.982
3	8	0	—	0.332	—	—	0.334
3	8	1	100	0.442	100	∞	0.451
3	8	2	100	0.551	100	∞	0.564
3	8	5	100	0.868	99.9984	61482	0.890
3	8	10	100	1.391	100	∞	1.421
3	8	20	100	2.448	99.9995	209201	2.475
3	8	48	100	5.596	100	∞	5.719

Table 6: Natural interference: ORPL (2Hz) vs. U.

	T-LOW		T-HIGH	
U	*PDR* (%)	*DC* (%)	*PDR* (%)	*DC* (%)
0	—	0.295	—	0.571
1	99.8	0.380	98.2	0.710
5	98.9	0.859	97.4	1.312
10	98.9	1.497	98.4	2.140
20	97.8	2.977	86.3	4.718
48	73.0	6.845	65.5	7.402

These trends are expected; however, Table 5 shows that, in the same conditions, Crystal performs significantly better, in line with [15]. Regardless of the $\langle N_T, W_T \rangle$ combination used, Crystal *always* achieves perfect *PDR*, even in the extreme $U=48$. In these experiments, not a single packet was lost of total 600k sent. This is largely to be ascribed to the excellent performance of the underlying Glossy layer (Table 7). Further, Crystal achieves a *DC* lower than ORPL, itself the best among the mainstream protocols considered. For instance, for $U=48$ the improvement is 18% with $N_T=3$, and 29% with $N_T=2$. With no data sent ($U=0$), the *DC* of ORPL is, however, comparable with $N_T=2$, and even lower than $N_T=3$.

Note how the Crystal sink is duty cycled, like other nodes; this is an asset in deployments where powering the sink is complicated. In contrast, the results shown throughout the paper for mainstream protocols use an always-on sink; we verified this provides them with highest *PDR* and lowest *DC*.

5.3 Natural Interference: T-HIGH

Next we discuss experiments assessing the same protocols during daytime, which presents higher levels of interference mostly arising from WiFi traffic, as discussed in §3.

Table 7: *PDR* of Glossy.

scenario	N_T,W_T	*PDR* (%)
T-LOW	2, 6	100
	3, 8	100
T-HIGH	2, 6	99.971
	3, 8	99.985
J-WIFI 1 jammer	3, 8	100
J-WIFI 6 jammers	3, 8	99.32
J-MWO 42	3, 8	99.88
J-MWO 13	3, 8	100
J-MWO 7	3, 8	67.90
J-MWO 7	6, 12	83.86
J-MWO 7	10, 17	99.76

Concerning the mainstream baseline protocols, Table 4 shows a generalized decrease in *PDR* accompanied by significant increases in *DC*. As in T-LOW, ORPL is the protocol with the best performance. The price to pay, however, is the nearly twofold *DC* increase for both 2 and 8Hz, as a result of longer idle listening and retransmissions induced by interference. Varying the number U of senders (Table 6) shows a similar trend of decreasing *PDR* and increasing *DC*.

Instead, Crystal performs quite well (Table 5). *PDR* is perfect or near-perfect regardless of the value of U; the occasional (4 out of total 700k) packet loss for some values of U is likely due to the unpredictable nature of T-HIGH. Further, *DC* is nearly identical to the T-LOW case. For instance, in the worst-case scenario of $N_T=3$ and $U=48$, the increase in T-HIGH w.r.t. T-LOW is a negligible 0.22%. This is partly ascribed to the inherent reliability of the Glossy protocol Crystal builds upon. However, our experiments also show that Glossy *by itself* does not achieve perfect *PDR*. The superior reliability of Crystal is due to its redundancy mechanisms built *atop* Glossy, overcoming daytime noise with little additional overhead. Another way to look at this is to observe that even in the configuration with $N_T=2$, i.e., less reliability in the Glossy layer, Crystal still achieves the same *PDR* as $N_T=3$, while of course enjoying better *DC*.

5.4 Generated Interference: J-WIFI

We turn our attention to noise patterns we can control via JamLab (§3). We first analyze a single J-WIFI jammer next to the sink, then 6 of them fully covering the network. We focus on $U=1$ as this is sufficient to draw the observations motivating the further work described in the next sections.

Single jammer next to the sink. We use a single jammer, node 7 in Figure 2; its placement is challenging, at only 1m from the sink. RPL shows a reasonable *PDR*=84%, while ORPL yields near-perfect *PDR* with both 2 and 8Hz, and a *DC* comparable to T-HIGH (Table 8). In the same conditions, Crystal achieves perfect *PDR* and lower *DC* than ORPL (Table 9). This remarkable performance is mainly a consequence of the perfect performance of Glossy (Table 7).

Six WiFi jammers covering the entire network. We next consider 6 JamLab nodes generating WiFi interference across the entire network like T-HIGH, but with significantly higher noise (§3). As RPL showed low performance even with a single jammer, we focus on ORPL, which has significant difficulty overcoming this noise

Table 8: Generated noise: Baseline, $U=1$.

	node ID	protocol	wake-up (Hz)	*PDR* (%)	*DC* (%)
J-WIFI	7	RPL	8	84	1.50
			2	89	1.30
	7	ORPL	8	99.7	1.31
			2	99.9	0.59
	6 jammers	ORPL	8	60	3.91
			2	64	1.70
J-MWO	42	ORPL	8	98.3	2.13
			2	98.6	0.844
	13	ORPL	8	99.7	1.84
			2	98.0	0.67
	7	ORPL	8	99.1	2.23
			2	99.8	0.67

Table 9: Generated noise: Crystal, $U=1$.

	node ID	N_T, W_T	R	*PDR* (%)	*DC* (%)
J-WIFI	7	3, 8	2	100	0.457
		2, 6	2	100	0.403
	6 jammers	3, 8	2	100	0.497
		2, 6	2	100	0.443
J-MWO	42	3, 8	2	100	0.507
		2, 6	2	99.52	0.430
	13	3, 8	2	100	0.459
		2, 6	2	100	0.405
	7	3, 8	2	78.5	0.453
		2, 6	2	78.6	0.425
	7	3, 8	6	100	1.11
	7	6, 12	2	100	0.839

level, regardless of the wake-up interval; in the best case, 2Hz achieves *PDR*=64% (Table 8).

Glossy achieves near-perfect *PDR* (Table 7), becoming perfect once combined with the Crystal mechanisms built atop, yielding a *DC* only 12% higher than T-LOW (Table 9). However, when $U > 1$ (results omitted due to space limitations) Crystal experiences a slight *PDR* decrease of 1–2%. The reason is that, with very high interference throughout the network, no alternate, good paths exist for packets to reliably reach the sink.

5.5 Generated Interference: J-MWO

We study the impact of a JamLab-emulated microwave oven, causing interference much stronger than WiFi and with different temporal patterns (§3). We move the jammer progressively closer to the sink, yielding increasingly challenging scenarios. Given the results in the previous section, our comparison against mainstream protocols considers only ORPL, as RPL yields unacceptable performance.

Jammer *far* from the sink, node 42. We first use a jammer on node 42, far from the sink, in a corner of the network, and amid a dense neighborhood; its noise affects neighboring nodes, but bears limited influence to the rest of the network.

ORPL performs well in this scenario (Table 8) although with a *DC* increased w.r.t. lower-noise scenarios. This is due to its buffering and continuous attempts to re-transmit packets until it finds the channel free (§4.2). Recall that the J-MWO scenario induces periods of strong interference alternated to periods with no interference (§2.2). Therefore, the buffering and infinite CCA retries in ORPL effectively delay packets when the microwave oven interference is active, enabling their transmission during no-interference periods. Nevertheless, these retransmissions do increase the *DC*.

Crystal instead achieves perfect *PDR* (Table 9). Nevertheless, the underlying Glossy layer is affected by interference (Table 7); therefore, reliability in Crystal comes at the cost of a higher *DC*. This cost is even higher than with 6 WiFi jammers, although in the latter case the *PDR* of Glossy is worse. The reason is the position of node 42; being in a corner of the network, its strong interference causes the loss of acknowledgments in that neighborhood, triggering retransmissions from the corresponding senders and unnecessarily keeping the *entire* network awake to help forwarding. Instead, in the scenario with 6 WiFi jammers covering the entire network, packet losses are spatially and temporally distributed, and the redundancy brought by both Glossy and Crystal enables packets to more easily find routes "around" the interference.

Jammer *close* to the sink, node 13. We now move the jammer to node 13 at ≈4m from the sink. Intuitively, this is likely to be more disruptive than the far away node 42, but less than an even closer placement, discussed next.

Yet, our results tell a different story. The *PDR* of ORPL is nearly perfect (Table 8) and achieved with a *DC* ≈20% lower w.r.t. node 42 above. The same holds for Crystal (Table 9), which achieves perfect *PDR* with a *DC* ≈9% lower w.r.t. node 42, thanks to the perfect reliability of Glossy (Table 7). This improved performance arises from jammer position. Node 13 is closer to the sink than 42 and induces stronger interference on it, but it is also more "central", allowing packets to follow routes "around" it. Instead, node 42 is in the network corner, where noise disruption is much harder to compensate via alternative routes.

Jammer *next* to the sink, node 7. When moving the J-MWO jammer on node 7, at 1m from the sink, the *PDR* of Crystal significantly degrades for the first time, causing a 21.5% packet loss (Table 9), mainly due to the fact that, unlike previous scenarios, the underlying Glossy layer loses 32.1% of the packets. The reason is that the interference on node 7 is so strong and so close that Glossy cannot overcome it. Receiving packets via alternate routes, as with node 13, is no longer an option because *all* routes are jammed by interference, given that the sink is basically at the center of it.

In contrast, ORPL achieves near-perfect *PDR* also in this case (Table 8) and with a *DC* only marginally different w.r.t. the interference source on node 13. From the point of view of ORPL, the two situations are virtually the same: *i)* both node 7 and 13 are in the center of the network, unlike the more challenging corner placement of node 42, and *ii)* in both cases, buffering and retransmissions guarantee that a packet not received by the sink due to interference is eventually received in the periods without it.

Instead, Crystal dissemination is designed to be as fast as possible, even with the redundancy it builds atop the even shorter one-shot Glossy floods. Consequently, Crystal and Glossy cannot exploit a "wait-and-see" strategy as in ORPL.

5.6 Is There a Better Configuration?

We study a configuration yielding perfect *PDR* in the worst scenario for synchronous transmissions, i.e., node 7 as J-MWO jammer. We explore two options: in Crystal, and in the underlying Glossy.

Crystal: Keeping the network awake. We observed that an asset of ORPL is that it can retransmit until interference ceases. The Crystal analogous comes from increasing R, i.e., the number of consecutive silent TA pairs detected before determining that communication is over and it is safe to enter sleep mode until the next epoch (§2.1). Increasing R keeps the network awake longer, even when the sink reports via its A slot that no packet arrived in the previous T slot. This gives senders more opportunities to attempt retransmission under interference. Indeed, Table 9 shows that R=6 enables perfect *PDR*. However, keeping the network awake for 3x longer than before causes a nearly 3-fold increase in *DC*.

Glossy: Increasing redundancy. An alternative is to make the underlying Glossy layer more reliable. The main knob to achieve this is to increase the number N of retransmissions during a flood, and increase the slot duration W to ensure the flood has enough time to complete (§2.1). We verified that, when pure Glossy is used in isolation, a setting $N=10$, $W=17$ yields *PDR*=99.76%. However, the reliability provided by Crystal atop Glossy enables the use of a smaller N, considerably reducing *DC*. Table 9 shows that with $N_T=6$, $W_T=12$, Crystal achieves perfect *PDR* (despite Glossy yielding only *PDR*=83.86%, see Table 7) but nearly doubles *DC*, as each packet is transmitted twice as many times w.r.t. $N_T=3$.

In summary, a proper *static* configuration of Crystal or Glossy parameters enables perfect reliability but with unacceptable power consumption w.r.t. ORPL (which however does *not* achieve perfect *PDR*). Ideally, perfect *PDR* should come without increasing significantly the *DC* observed in the other scenarios in Table 9, i.e., at most 0.50%. Further, over-provisioning for the worst case, as these static configurations do, is undesirable. Ideally, Crystal should *dynamically* adapt to interference, bearing extra energy costs only when needed.

6 TAMING STRONG INTERFERENCE

We illustrate a technique to *escape* interference and a complementary one to *fight* it after detecting its presence.

Escaping Interference: Channel Hopping. Exploiting frequency diversity is a well-known technique for interference resilience. Interference usually affects only some of the 16 channels available in IEEE 802.15.4 (§2.2). Therefore, a channel-hopping sequence can be used network-wide to enable subsequent TA pairs to move to different channels, reducing the probability that two consecutive ones both execute on noisy channels. This simple modification does not affect any Crystal parameters.

Channel hopping is driven by the S phase (Figure 5); the channels of TA pairs in the epoch depend on the S channel, itself based on a predefined sequence. This mechanism realigns all nodes to the same channel at the epoch start, independent of the number of TA phases they executed in the previous one.

A key decision is which channel to use next. WiFi and microwave ovens are common noise sources, jamming 4 and 7 adjacent channels, respectively (§2.2). Spacing the current and next channel apart by 4 channels is sufficient to escape WiFi, but not microwave ovens. Therefore, our implementation uses a hopping sequence with 7-channel spacing; alternate hopping sequences can exploit a priori knowledge about interference. Notably, selecting the number of channels to hop over requires little knowledge compared, e.g., to approaches that probe the environment and limit themselves to channels with the least interference [28].

Fighting Interference: Noise Detection. Our next technique relies on the ability to detect abnormally high noise levels. Recall from §2.1 that, in Crystal, the distributed termination condition relies on counting *silent pairs* and missed acknowledgements. Under high noise, these *missing-packet* conditions often occur even when a packet was transmitted, but encountered interference. If noise strikes during the T phase close to the sink, the sender will re-transmit the packet in the next T slot. If the sink still does not receive the packet in R consecutive T slots, it mistakenly detects termination and puts the whole network to sleep. Instead, noise in the network periphery may cause a node to similarly miss Z acknowledgements and go to sleep, likely before the sink. In both cases, data may remain un-delivered because termination was falsely detected.

Adding noise detection and changing termination conditions fights these cases. Noise detection can be easily achieved by periodically checking the CCA pin of CC2420; in our implementation, all nodes perform the CCA every 64μs while listening during T or A phases, and define high noise when $RSSI > -60$dBm is detected at least 80 times. This threshold is designed to detect only very high noise, e.g., a microwave oven; lower thresholds would unnecessarily trigger the scheduling of extra TA pairs, e.g., in the WiFi scenarios of §5, where even the unmodified Crystal achieves perfect reliability.

As for distributed termination, intuitively, in the presence of noise missing packets do not count towards termination, keeping the network awake and allowing more opportunities for data and acknowledgments to escape the interference. Recall that receiving any packet keeps a node awake to serve as a forwarder. We make the following modifications to Crystal:

- define R_{noise} as the maximum number of *consecutive* slots *i)* without a packet *and ii)* with high noise.
- change the termination rule at the sink; the network goes to sleep when *either i)* R non-noisy no-data T slots occur since the last received data, *or ii)* $max(R, R_{noise})$ consecutive noisy no-data T slots occur.
- change the termination rule elsewhere; a node goes to sleep when *either i)* it receives a sleep command from the sink, *or ii)* it detects Z non-noisy no-data slots since the last packet received in T or A, *or iii)* $max(Z, R_{noise})$ consecutive noisy, silent A slots occur.

We empirically determined that R_{noise}=6 strikes a good balance between reliability and energy consumption.

Fighting *and* Escaping Interference. Although both these techniques improve performance along some dimension, it is only

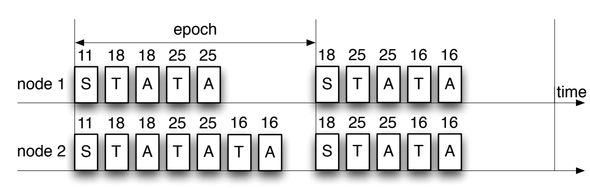

Figure 5: Channel hopping in Crystal. The number on each Crystal phase denotes the channel used.

through their combination that very strong interference can be effectively overcome with very low energy consumption, as shown next. Indeed, frequency diversity reduces the probability of the sink to be exposed, in consecutive TA pairs, to high noise levels from the same source, mitigating the above drawback of noise detection. On the other hand, the ability to detect and react to noise is helpful in reducing packet loss when hopping from one bad channel to another one.

7 UNDER STRONG INTERFERENCE

We now evaluate the techniques in §6 and show that they not only overcome the interference scenarios considered in §5, but also sustain much higher noise levels, detailed next.

7.1 Experimental Setup

We extend our experimental setup along two dimensions.

Channel mapping. Testing our channel hopping mechanism in principle requires reproducing interference across multiple channels, something JamLab cannot do (§2.2). We overcome this limitation via a *mapping* between the 16 channels of IEEE 802.15.4 and those in the testbed. Whenever our channel hopping mechanism decides to switch to a channel c, a corresponding channel c_{real} is instead used for communication, based on a predefined mapping $c \to c_{real}$ based on the interference types and channels affected we want to reproduce. For instance, when emulating a microwave oven, we map channels 20–26 to the real one used by J-MWO jammers.

More challenging interference scenarios. As described later, extending CRYSTAL with the techniques in §6 allows it to sustain much stronger interference than the one in §5, which considered the *separate* effect of generated J-WIFI and J-MWO interference. Therefore, we now focus on the *combined* effect of these two interference types. We combine them in two ways, yielding the scenarios in Table 10. The first, COMBINED$_{split}$, combines the two types of interferences by placing each on different real channels. This significantly reduces the chances that channel hopping finds a good channel, and increases the likelihood to hop from one type of interference to the other. The second scenario, COMBINED$_n$, is even more challenging, placing J-MWO and J-WIFI jammers on the *same* real channel, generating noise that is the *sum* of the two. Increasingly challenging scenarios can be generated by determining the number n of channels this strong interference is mapped to. Table 10 shows we experiment with n ranging from 7 (i.e., when J-MWO and J-WIFI fully overlap) to 16 (i.e., *all* channels jammed by the same combined interference).

Besides combining interference types, we also strengthen J-MWO, the most disruptive one, by using 2 jammers simultaneously, the worst in §5: node 7 next to the sink, and node 42 in the corner. As for J-WIFI, using the scenario with 6 jammers would force us to remove 8 nodes in total, further reducing the network size. Therefore, we used 4 J-WIFI jammers that, we verified, yield a noise pattern close to natural T-HIGH.

As mentioned at the end of §3, we use the resulting 43-node network across all scenarios. To re-establish our ORPL baseline, Table 11 (left) reports experiments with 4 J-WIFI, 2 J-MWO, and their combination over a single channel. ORPL performance is good also with 2 J-MWO, but degrades significantly even with only 4 J-WIFI jammers, instead of the 6 used in §5.4.

Table 10: Scenarios with combined interference generated by 2 J-MWO and 4 J-WIFI.

scenario	#channels jammed		description
	2 J-MWO	4 J-WIFI	
COMBINED$_{split}$	7	6	jammers on different *real* channels based on type, mapped on different sets of channels
COMBINED$_n$	$n \in \{7, 10, 13, 16\}$		all jammers on one *real* channel, itself mapped on n channels

Table 11: ORPL (2Hz) in a 43-node network, $U=1$.

scenario	TX Power 0 dBm		TX Power −7 dBm	
	PDR (%)	*DC* (%)	*PDR* (%)	*DC* (%)
T-LOW	99.6	0.497	97.0	0.454
T-HIGH	98.5	0.776	–	–
4 J-WIFI	61.0	1.35	39.5	6.192
2 J-MWO	97.8	1.19	94.8	1.503
2 J-MWO 4 J-WIFI	65.0	2.14	39.6	5.375

7.2 Channel Hopping

We are now ready to study CRYSTAL extended with channel hopping as discussed in §6. We call this variant CRYSTAL^{CH}, to distinguish it from the original single-channel one, and call CRYSTAL$^{CH}_{ND}$ the variant that also adds noise detection.

Table 12 reports experiments under natural T-HIGH interference, without channel mapping and with CRYSTAL^{CH} hopping across all 16 channels. A comparison with Table 5 shows that CRYSTAL achieves perfect *PDR* (no packets lost of total 150k sent) regardless of U, and does so with $N_T=2$, which generally yields worse *PDR* w.r.t. $N_T=3$. Further, *DC* is 1–2% lower than the single-channel version under T-HIGH.

Table 12: CRYSTAL^{CH}, under T-HIGH.

N_T	U	*PDR* (%)	*DC* (%)
2	0	–	0.294
2	1	100	0.392
2	2	100	0.486
2	5	100	0.766
2	10	100	1.221
2	20	100	2.122
2	48	100	4.906

A bigger question lingering from §5 is whether CRYSTAL^{CH} can overcome J-MWO interference next to the sink. We first analyze the performance in the COMBINED$_{split}$ scenario (Table 13). Recall this subsumes the scenario with J-MWO on node 7 (end of §5) by adding a second jammer on node 42, defining a much more challenging setup. Indeed, when hopping out of J-MWO interference, found with a $\frac{7}{16}=43.75\%$ probability, there is still a 37.5% chance to stumble on J-WIFI interference, and only a 18.75% chance to enjoy T-LOW interference. Nevertheless, CRYSTAL^{CH} achieves perfect *PDR* for $U=1$ and three-nines reliability for $U>1$, $N_T=3$. Further, this is achieved with only a slight increase in *DC* w.r.t. our lowest-interference scenario, T-LOW: 14.3% and 12.6% for $N_T=2$ and $N_T=3$, respectively.

The next step is to identify the limit of CRYSTAL^{CH}, which clearly depends on the type of interference applied and number of channels affected. Table 15 explores this limit by using the COMBINED$_n$ scenario of Table 10. The interference is stronger, as it is the *sum* of 2 J-MWO *and* 4 J-WIFI, which in Table 13 are instead split on

Table 13: CRYSTAL$^{\mathrm{CH}}$, under COMBINED$_{split}$.

N_T	U	*PDR* (%)	lost 1 pkt in	*DC* (%)
2	0	—	—	0.335
2	1	100	∞	0.454
2	2	100	∞	0.583
2	5	99.949	1980	0.954
2	10	99.982	5620	1.568
2	20	99.979	4822	2.792
2	42	97.627	42	5.646
3	0	—	—	0.374
3	1	100	∞	0.514
3	2	100	∞	0.661
3	5	99.952	2086	1.069
3	10	99.988	8374	1.750
3	20	99.941	1681	3.138
3	42	100	∞	6.434

Table 14: CRYSTAL$^{\mathrm{CH}}_{\mathrm{ND}}$, under COMBINED$_{16}$.

N_T	U	*PDR* (%)	lost 1 pkt in	*DC* (%)
2	0	—	—	0.543
2	1	99.230	130	0.734
2	2	99.120	114	0.948
2	5	98.777	82	1.622
2	10	98.732	79	2.803
2	20	98.582	71	5.372
2	42	90.056	10	9.308
3	0	—	—	0.739
3	1	99.515	206	0.927
3	2	99.361	157	1.145
3	5	98.914	92	1.693
3	10	98.394	62	2.825
3	20	96.640	30	5.206
3	42	94.397	18	9.952

Table 15: CRYSTAL$^{\mathrm{CH}}$ vs. CRYSTAL$^{\mathrm{CH}}_{\mathrm{ND}}$, under COMBINED$_n$.

			CRYSTAL$^{\mathrm{CH}}$			CRYSTAL$^{\mathrm{CH}}_{\mathrm{ND}}$		
n	N_T	U	*PDR* (%)	lost 1 pkt in	*DC* (%)	*PDR* (%)	lost 1 pkt in	*DC* (%)
7	2	0	—	—	0.328	—	—	0.367
7	2	1	100	∞	0.444	100	∞	0.487
7	2	10	100	∞	1.574	100	∞	1.624
7	2	20	100	∞	2.746	100	∞	2.890
7	2	42	100	∞	5.848	100	∞	5.936
7	3	0	—	—	0.370	—	—	0.444
7	3	1	100	∞	0.501	100	∞	0.576
7	3	10	100	∞	1.749	100	∞	1.826
7	3	20	100	∞	3.142	100	∞	3.256
7	3	42	100	∞	6.494	100	∞	6.566
10	2	0	—	—	0.347	—	—	0.430
10	2	1	94.439	18	0.458	99.919	1237	0.544
10	2	10	71.201	3	1.289	99.962	2637	1.911
10	2	20	46.900	2	1.511	99.788	471	3.414
10	2	42	22.459	1	1.618	99.557	226	7.008
10	3	0	—	—	0.386	—	—	0.521
10	3	1	93.262	15	0.512	99.919	1230	0.660
10	3	10	74.722	4	1.469	99.646	282	2.130
10	3	20	54.497	2	1.878	99.252	134	3.730
10	3	42	30.353	1	2.271	98.402	63	7.464
13	2	0	—	—	0.362	—	—	0.483
13	2	1	84.992	7	0.467	99.748	397	0.621
13	2	10	36.581	2	0.844	99.719	356	2.322
13	2	20	19.497	1	0.817	99.409	169	4.132
13	2	42	9.277	1	0.882	97.577	41	8.456
13	3	0	—	—	0.410	—	—	0.628
13	3	1	85.775	7	0.522	99.919	1237	0.696
13	3	10	47.427	2	1.073	98.608	72	2.484
13	3	20	26.522	1	1.121	96.853	32	4.255
13	3	42	13.936	1	1.230	97.360	38	8.436

separate sets of channels. Moreover, we apply this strong interference to an increasing number n of channels, progressively reducing the options to hop away from interference. Table 15 (left) shows that when n=7, CRYSTAL$^{\mathrm{CH}}$ achieves perfect *PDR* regardless of N_T and number U of senders, with a *DC* marginally smaller than in COMBINED$_{split}$. However, when only 6 channels are free and the others subjected to COMBINED$_{10}$ interference, performance drastically drops. With U=1 sender active, *PDR*=94% is achieved at best, with N_T=3; as U increases, *PDR* plummets. Finally, with only 3 channels free reliability reaches an unacceptable *PDR*<85% with U=1, and at best *PDR*=13.9% with all U=42 senders.

7.3 Channel Hopping *and* Noise Detection

These scenarios are very challenging, both in absolute terms and w.r.t. the literature, making the performance of CRYSTAL$^{\mathrm{CH}}$ already remarkable. Nevertheless, we can push reliability even further. When interference affects so many channels that it becomes difficult to *escape* it, the only other choice to improve reliability is to *fight* it with noise detection (§6).

Indeed, starting from 10 channels jammed, unlike the channel hopping alone, its combination with the noise detection (Table 15, right) achieves two- to three-nines *PDR* with U=1. For U>1 the performance gain is even more visible as CRYSTAL$^{\mathrm{CH}}_{\mathrm{ND}}$ achieves *PDR*>96.8% even with 13 channels jammed.

Noise detection becomes more important as the number n of jammed channels increases. The extreme case is when *all* channels are jammed by the same strong interference (Table 14); channel hopping becomes pointless and reliability is provided entirely by noise detection, which performs quite well. Indeed, the *PDR* achieved here is only marginally lower than in COMBINED$_{13}$, with the worst-case U=42 achieving *PDR*=90%. To put this value in context, we observe that it is *i)* comparable with what RPL achieves in T-LOW with U=1 (Table 4), and *ii) more* than what ORPL achieves in the natural T-HIGH (no microwave ovens) with U=20 (Table 6).

The price to pay for this remarkable reliability is energy consumption. A drawback of noise detection is that high noise keeps the network awake even without packet transmissions (§6). This is reflected in the *DC* increase as the number n of jammed channels increases, which increases the likelihood of remaining unnecessarily awake. This is clearly undesirable for U=0; yet, it is key to reliability as U increases, as seen by comparing the two sides of Table 15. The actual impact of this increased *DC* on the overall energy consumption depends on the aperiodic traffic at hand, as we analyze in §7.5.

On the other hand, we also verified that under T-HIGH, unlike the extremely challenging scenario above, the *DC* of CRYSTAL$^{\mathrm{CH}}_{\mathrm{ND}}$ does not increase w.r.t. CRYSTAL$^{\mathrm{CH}}$ (Table 12) since interference is never strong enough to trigger our noise detection mechanism.

7.4 A Different Topology: Low Power

We present results with the lower transmission power of −7dBm. This reduces the number of neighbors and increases network diameter (Figure 4), yielding a more challenging topology.

To re-establish the ORPL baseline, we repeated experiments in the new topology (Table 11, right). ORPL performs close to the high-power setting with only minimal (T-LOW) or J-MWO interference, but shows drastic performance degradation in the presence of J-WIFI, with an almost halved *PDR*.

We ran several CRYSTAL experiments, confirming the trends hitherto observed. However, *DC* increases slightly in all cases, as we must use larger Glossy slots to handle the larger network diameter

Table 16: Low power: CRYSTAL$^{\text{CH}}_{\text{ND}}$.

	COMBINED$_{split}$				COMBINED$_{16}$			
U	N_T	*PDR* (%)	lost 1 pkt in	*DC* (%)	N_T	*PDR* (%)	lost 1 pkt in	*DC* (%)
0	3	—	—	0.541	4	—	—	1.072
1	3	99.992	11825	0.709	4	99.603	252	1.340
2	3	100	∞	0.865	4	99.218	128	1.696
5	3	100	∞	1.335	4	98.736	79	2.646
10	3	99.997	28889	2.125	4	97.640	42	4.194
20	3	99.987	7840	3.652	4	95.082	20	7.784
42	3	100	*Inf*	7.612	4	93.146	15	14.982

(Table 2). Due to space limitations, we focus only on CRYSTAL$^{\text{CH}}_{\text{ND}}$ in the final, most challenging scenarios.

Table 16 (left) shows results in the COMBINED$_{split}$ scenario. Comparing against Table 13 we see that N_T=3 achieves a *PDR* similar to the high-power case. However, to sustain the most challenging scenario COMBINED$_{16}$ with all channels jammed, the redundancy of the underlying Glossy must be increased to N_T=4 (Table 16, right). This enables CRYSTAL$^{\text{CH}}_{\text{ND}}$ to achieve a *PDR* within 0.5–3% of the high-power case: above 93% even with all 42 concurrent senders.

These results confirm the effectiveness of our techniques also in the larger-diameter, lower-power setting considered.

7.5 Back to Aperiodic Data Collection

We now reconcile the experimental results reported with the original goal of supporting aperiodic, sparse data collection.

We use the traffic profile in Table 1 and adapt it for missing values of U in our experiments, replaced by the next higher value available. For instance, the value 606 for U=5 is actually the sum of the epochs with 3, 4, or 5 senders present. This yields worst-case estimates of *PDR* and *DC*, as both increase with U. These are aggregated over the entire dataset as

$$C = \frac{\sum_{u=0}^{N} c(u) \times e(u)}{\sum_{u=0}^{N} e(u)}$$

where $c(u)$ is the value of *PDR* or *DC* for a given number u of concurrent senders (reported in previous sections) and $e(u)$ is the number of epochs in which u concurrent senders are present (from Table 1). As the the original dataset uses an epoch E=30s, we rescaled *DC* accordingly (i.e., $\frac{1}{3}$ of those hitherto shown) to enable a comparison with the performance reported in [15], albeit in a different testbed. In our results (Table 17), due to space limitations, we consider only the extremes of the interference scenarios we analyzed in the paper, viz. natural interference and generated interference in the COMBINED$_{16}$ scenario. These are however sufficient to draw a few interesting observations.

First, in the T-LOW scenario $DC \approx 0.1\%$; this confirms that our results are in line with the per-mille *DC* originally reported in [15]. Interestingly, this is identical to daytime (T-HIGH) when instead the original CRYSTAL behaved erratically, as quoted in §1. This confirms that the techniques presented in this paper effectively combat interference without sacrificing ultra-low power consumption.

Finally, Table 17 shows that the *PDR* accrued over the 36-day dataset remains near to 99.5% in COMBINED$_{16}$, which is remarkable given the very challenging nature of this interference scenario.

Table 17: CRYSTAL$^{\text{CH}}_{\text{ND}}$: performance with the aperiodic, sparse, real-world traffic profile shown in Table 1.

interference scenario	N_T=2 *PDR*	N_T=2 *DC*	N_T=3 *PDR*	N_T=3 *DC*
T-LOW	100	0.105	100	0.119
T-HIGH	100	0.105	—	—
COMBINED$_{16}$	99.487	0.198	99.592	0.263

Further, this is achieved with $DC \approx 0.2\%$ depending on N_T. This is twice the baseline established by natural interference, but in absolute terms it is remarkably small w.r.t. the energy consumption commonly reported in the state of the art.

8 RELATED WORK

We survey approaches that share our goal of making multi-hop protocols for low-power wireless communication resilient to environmental interference. Interference has also been studied from a security perspective by identifying several types of jamming attacks and related countermeasures. Although not directly related to our contribution, these techniques may inspire alternate resilience mechanisms; we refer the interested reader to [19].

CSMA + Channel Hopping. Adding channel hopping to combat interference is well accepted in the literature, with recent works modifying standard, CSMA protocol stacks. MiCMAC [20] extends ContikiMAC with channel hopping, resulting in a synchronization-free MAC with high *PDR* under WiFi interference. MiCMAC mechanisms require transmitting and receiving nodes to synchronize in time as well as across channels, increasing latency. Oppcast [18] and MOR [28] offer full-stack alternatives to RPL and MicMAC, combining channel hopping and opportunistic routing to combat high latencies while also escaping high interference.

As MOR code is not available, we offer an informal, numerical comparison with the evaluation in [28], performed on FlockLab with WiFi on one channel and an effective U=2.1. Using this jammed channel plus two free ones, MOR shows the best results: *PDR*=99.35% and *DC*=1.56%. We compare to a more challenging scenario with constant, generated WiFi traffic on all channels in our testbed where CRYSTAL shows *PDR*=100% and *DC*=0.559 for U=2. This *DC* is nearly *three times smaller* w.r.t. MOR, and achieved without any interference avoidance mechanisms. Naturally, with more concurrent packets, the *DC* of CRYSTAL increases, however the same is true for other protocols. Further, in the absence of traffic, a common case in §7.5, CRYSTAL maintains $DC < 0.4\%$, levels that duty cycling protocols cannot achieve due to required periodic channel probing. Finally, to manage latency, these protocols hop among few channels, selected during pre-deployment evaluations. In contrast, CRYSTAL$^{\text{CH}}$ can use all channels without affecting its performance, allowing it to adapt to changing interference.

TDMA + Channel Hopping. TSCH [26] with Orchestra [5] scheduling offers a protocol in which all nodes follow a repeating, slotted schedule, with local and independent slot allocation. The number and type of slots is statically determined, according to expected traffic. Results from Indriya show Orchestra with 47 slots maintains *PDR*=99.99% with an average *DC*=0.4%, without interference; in an analogous setting, CRYSTAL consumes twice as much, *DC*=0.8%. However, in Orchestra the duty cycle of nodes varies significantly across the network, with nodes closer to the sink reporting much higher values. Further, Orchestra is designed for periodic data, which is critical to statically configure slot parameters. In the aperiodic, dynamic scenarios considered in §7.5, Orchestra would overdimension for the worst case, unable to reduce *DC* under low traffic. Finally, Orchestra has not been evaluated under interference.

Synchronous Transmissions + Channel Hopping. The combination of channel hopping and synchronous transmissions has also been used to increase parallelism for bulk data dissemination in Splash [2] and Pando [3]. Both protocols also see improvements due to diverse noise levels across channels, but their approaches are not competitive at low data rates.

In the context of the EWSN dependability competition [23], the three winning approaches in 2017 [7, 17, 21] perform channel hopping *inside* Glossy, a contrast to the noise resilience mechanisms we designed *on top* of Glossy. However, these solutions were highly specialized for the (single-sender) competition scenario and are not immediately reusable towards our goals. Instead, we evaluated $\text{Crystal}_{\text{ND}}^{\text{CH}}$ with concurrent senders and in a wide range of intense interference. Analyzing and exploiting the interplay between Glossy-level channel hopping and our Crystal-level techniques is intriguing, but is beyond the scope of this paper, albeit in our short-term research plans.

9 CONCLUSIONS AND FUTURE WORK

This paper set out to evaluate Crystal's ability to sustain aperiodic, sparse traffic under strong interference. As Crystal relies on Glossy, we also offer a noise resilience evaluation for it, along with the two mainstream protocols, RPL and ORPL, we chose as baselines.

Unlike existing works limited to natural WiFi interference, we subjected these protocols also to the stronger noise generated by JamLab-emulated microwave ovens, which exhibit different interference patterns similar to those found in real environments. In our reproducible and controlled setup we showed, for the first time, that ORPL is very resilient to this type of interference, while Crystal is not. This motivated us to extend it with a combination of channel hopping and noise detection. We showed that our enhanced $\text{Crystal}_{\text{ND}}^{\text{CH}}$ protocol achieves unprecedented, near-perfect reliability even against the combination of emulated WiFi and microwave ovens, along with a per-mille duty cycle in the aperiodic, sparse traffic targeted by Crystal.

Regarding future work, a promising avenue is to distill the knowledge gained from the experimental campaigns presented in this paper into models able to identify the proper Crystal configuration given a known or estimated pattern of interference; this could potentially inform and greatly simplify in-field system configuration.

Furthermore, our work shows that effective strategies to overcome interference can be implemented *atop* Glossy, in contrast with the current trend of incorporating them *inside* it. A design similar to ours could be applied, in principle, to other Glossy-based systems (e.g., [9], [16]). However, a more fundamental research question, implicitly opened by this paper, concerns the tradeoffs between the two approaches; further study is required to identify under which conditions the techniques considered are more effective if implemented atop Glossy or, vice versa, inside it. The answer to this question could enable a novel design combining both approaches, yielding unprecedented levels of resilience to interference.

The source code of Crystal is freely available as open source at `https://github.com/d3s-trento/crystal`.

10 ACKNOWLEDGEMENTS

This work is partially supported by the CrystalClear project funded through the EU H2020 project WiSHFUL (grant agreement n. 645274), and by the Approxim@ction project funded by EIT Digital.

REFERENCES

[1] C. A. Boano et al. JamLab: Augmenting sensornet testbeds with realistic and controlled interference generation. *Proc. of IPSN*, 2011.
[2] M. Doddavenkatappa, M. Chan, and B. Leong. Splash: Fast Data Dissemination with Constructive Interference in Wireless Sensor Networks. In *Proc. of NSDI*, 2013.
[3] W. Du et al. When Pipelines Meet Fountain: Fast Data Dissemination in Wireless Sensor Networks. In *Proc. of SenSys*, 2015.
[4] A. Dunkels. The ContikiMAC radio duty cycling protocol. Technical Report T2011:13, SICS, 2011.
[5] S. Duquennoy et al. Orchestra: Robust Mesh Networks Through Autonomously Scheduled TSCH. In *Proc. of SenSys*, 2015.
[6] S. Duquennoy, O. Landsiedel, and T. Voigt. Let the tree bloom: Scalable opportunistic routing with ORPL. In *Proc. SenSys*, 2013.
[7] A. Escobar et al. Competition: RedFixHop with Channel Hopping. In *Proc. of EWSN*, 2017.
[8] F. Ferrari et al. Efficient Network Flooding and Time Synchronization with Glossy. In *Proc. of IPSN*, 2011.
[9] F. Ferrari et al. Low-power wireless bus. In *Proc. of SenSys*, 2012.
[10] O. Gnawali et al. Collection tree protocol. In *Proc. of SenSys*, 2009.
[11] O. Gnawali and D. Han. Performance of RPL under wireless interference. *IEEE Communications Magazine*, 51(12), 2013.
[12] A. Hithnawi et al. Understanding the impact of cross technology interference on IEEE 802.15.4. In *Proc. of WiNTECH*, 2014.
[13] N. Hung, H. Jeung, and K. Aberer. An evaluation of model-based approaches to sensor data compression. *IEEE TKDE*, 25(11), 2013.
[14] Intel Research Lab. http://db.csail.mit.edu/labdata/labdata.html.
[15] T. Istomin et al. Data prediction + synchronous transmissions = ultra-low power wireless sensor networks. In *Proc. of SenSys*, 2016.
[16] O. Landsiedel et al. Chaos: Versatile and Efficient All-to-all Data Sharing and In-network Processing at Scale. In *Proc. of SenSys*, 2013.
[17] R. Lim et al. Competition: Robust Flooding using Back-to-Back Synchronous Transmissions with Channel-Hopping. In *Proc. of EWSN*, 2017.
[18] M. Mohammad et al. Oppcast: Exploiting spatial and channel diversity for robust data collection in urban environments. In *Proc. of IPSN*, 2016.
[19] A. Mpitziopoulos, D. Gavalas, C. Konstantopoulos, and G. Pantziou. A survey on jamming attacks and countermeasures in WSNs. *IEEE Communications Surveys and Tutorials*, 2009.
[20] B. A. Nahas et al. Low-power listening goes multi-channel. In *Proc. of DCOSS*, 2014.
[21] B. A. Nahas and O. Landsiedel. Competition: Towards Low-Power Wireless Networking that Survives Interference with Minimal Latency. In *Proc. of EWSN*, 2017.
[22] U. Raza, A. Camerra, A. Murphy, T. Palpanas, and G. Picco. Practical data prediction for real-world wireless sensor networks. *IEEE Trans. on Knowledge and Data Engineering*, 27(8):2231–2244, 2015.
[23] M. Schuß et al. A competition to push the dependability of low-power wireless protocols to the edge. In *Proc. of EWSN*, 2017.
[24] M. Suzuki et al. Low-power, end-to-end reliable collection using Glossy for wireless sensor networks. In *Proc. of VTC Spring*, 2013.
[25] T. Winter et al. RPL: IPv6 Routing Protocol for Low-Power and Lossy Networks. RFC 6550, IETF, 2012.
[26] WPAN Working Group. 802.15.4-2015: IEEE standard for low-rate wireless networks. 2015.
[27] D. Yuan et al. Making 'Glossy' networks sparkle: Exploiting concurrent transmissions for energy efficient, reliable, ultra-low latency communication in wireless control networks. In *Proc. of EWSN*, 2014.
[28] P. Zhang et al. MOR: Multichannel Opportunistic Routing for Wireless Sensor Networks. In *Proc. of EWSN*, 2017.